

In: **Equine Respiratory Diseases**, P. Lekeux (Ed.)

Publisher: International Veterinary Information Service (www.ivis.org), Ithaca, New York, USA.

Diagnosis of Equine Respiratory Disease: Postmortem Methods and Lesion Interpretation (28-Apr-2003)

R. F. Slocombe

Veterinary Pathology, School of Veterinary Science, University of Melbourne, Werribee, Victoria, Australia.

Warning

This article contains specific details and illustrations of a postmortem dissection of a horse, and the text and illustrations may be confronting and offensive. The illustrations are all from postmortem cases and are intended to demonstrate how a detailed postmortem evaluation of the respiratory tract is conducted. The basis for interpretation of lesions is outlined and causes for these lesions reviewed.

Introduction

A thorough investigation of the respiratory tract in horses is a major undertaking, although it can be accomplished with minimal equipment. A targeted investigation of respiratory disorders is greatly enhanced by prior knowledge of antemortem clinical disease. Some changes at death may give a misleading impression of respiratory disease and the presence of serous to serosanguinous discharges at the nares is not pathognomonic. Many horses are euthanased by barbiturate over-dosage, and this frequently leads to pulmonary edema and discharges of edematous fluid from the nares after death. While fetid odor from the oral cavity may occur with pneumonias, particularly if gangrenous, it also commonly occurs in horses with gastrointestinal disease and as well as those in renal failure.

Knowledge of antemortem clinical signs also allows the prosector to reasonably assess risk of zoonotic disease, and the need for additional samples to isolate infectious agents. There is no single best way to approach postmortem of horses, but there is general agreement that adoption of a standardised method of dissection is best, since familiarity with normal structures enables better detection of subtle changes. Veterinary schools and diagnostic laboratories generally have well developed internal documents describing the procedures necessary for postmortem dissection in the horse, but these are seldom published and the publication by Sack and Habel [1] remains the most useful some 35 years after initial publication.

Establishing the Display Stage of Dissection

1. Initial Dissection - At this institution, horses are placed in right lateral recumbency. This enables best access for review of abdominal viscera, including spleen and cecum, but offers no particular advantage over other positions for examination of the respiratory tract. With the animal placed in left lateral recumbency, a midline ventral skin incision from mandible to inguinal region is made, and the upper legs dissected free from the body. A V-shaped incision is then made in the ventral aspect of the mandible, dissecting along both sides of the tongue and the tongue "dropped". (Fig. 1, Fig. 2 and Fig. 3).



Figure 1. Incision along the ventral midline of the neck joins a V-shaped incision along the inside of the mandible to enable removal of the tongue from the oral cavity. - To view this image in full size go to the IVIS website at www.ivis.org . -



Figure 2. Closer view of oral cavity with the tongue "dropped". - To view this image in full size go to the IVIS website at www.ivis.org . -



Figure 3. Inspection of the oral cavity and oropharynx. - To view this image in full size go to the IVIS website at www.ivis.org . -

In animals with narrow intermandibular angles, or where *rigor mortis* is especially strong, dissection of the floor of the mouth and tongue may be difficult unless the left (upper) mandible is sectioned with a saw just distal to the mandibular symphysis. (Fig. 4). This allows greater access to the lateral attachments of the tongue.



Figure 4. Placement of the saw cut in the upper mandible immediately caudal to the symphysis. In this case the tongue has already been "dropped". - To view this image in full size go to the IVIS website at www.ivis.org . -

2. Oral Cavity and Pharynx - The two incisions beginning at the point of the mandible are extended caudally to the level of the pharynx. The root of the tongue is held in place by hyoid bones and lateral pillars of the pharynx. With the tongue pulled ventrally, enabling visualisation of the oral cavity, incisions are continued along the lateral walls of the pharynx, until the hyoid bones become palpable. (Fig. 5, Fig. 6 and Fig. 7).



Figure 5. Lines of dissection of the lateral walls of the pharynx. - To view this image in full size go to the IVIS website at www.ivis.org . -



Figure 6. Placement of the knife to dissect the lower pharyngeal and laryngeal attachments from the ramus of the mandible. - To view this image in full size go to the IVIS website at www.ivis.org . -



Figure 7. Transverse incision of the soft palate to free this region of the pharynx from the roof of the mouth. - To view this image in full size go to the IVIS website at www.ivis.org . -

Although the hyoid bones can be severed with bone cutters, in older horses these bones are often brittle and when cut, can fracture leaving extremely sharp chisel-like bone ends which are a hazard for the prosector. Therefore, good practice is to sever the hyoid bones at their cartilaginous attachments to the larynx. In most animals, this can easily be achieved using a standard dissecting knife, leaving the ends of the hyoid bones covered with a cap of fibrocartilage and not a risk for the prosector. (Fig. 8).



Figure 8. Dissection of the hyoid bones from the larynx. By sliding the knife under the hyoid bone, the hyoid bone can be separated at its cartilaginous articulation (arrow). - To view this image in full size go to the IVIS website at www.ivis.org . -

By gently pulling downwards on the tongue, the dorsal aspect of the pharynx can be visualised and severed, freeing the tongue and pharyngeal tissues from the skull. (Fig. 9, Fig. 10). This is also the best time to evaluate the guttural pouches, because later in dissection the pouches may fill with fluids draining from other parts of the body and lesions become obscured.



Figure 9. Removal of tongue, pharynx and larynx (still attached to trachea) allows visualisation of guttural pouches. - To view this image in full size go to the IVIS website at www.ivis.org . -



Figure 10. Closer view of normal guttural pouch. - To view this image in full size go to the IVIS website at www.ivis.org . -

3. Cervical Trachea - Deep dissection of the ventral aspects of the neck allows isolation and separation of the esophagus and trachea from other ventral neck tissues. Once this is achieved, the trachea is occluded to ensure the lungs do not collapse upon opening the thorax. The means of occlusion is not important, and past practice at this institution was to have a range of large wooden stoppers, 10 to 15 cm in length and of varying diameters, which could be placed in the trachea via a tracheostomy incision, and then held firmly in place by heavy string ligatures. For various reasons, we have discontinued this practice, and now routinely clamp the trachea with 2 or 3 large gut clamps. This is much simpler and more effective at maintaining an adequate seal. (Fig. 11). Tracheal occlusion should take place near the thoracic inlet, avoiding structures in the proximal neck, such as the thyroids and salivary glands, or lymph nodes.

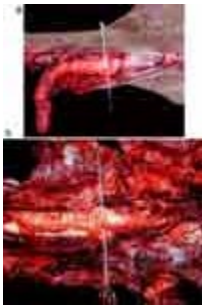


Figure 11. a) Occlusion of the trachea with large gut clamps prior to opening the thorax. b) Closer view of tracheal clamps. - To view this image in full size go to the IVIS website at www.ivis.org . -

At this stage of dissection, any gross lesions in the oral cavity, pharyngeal tissues, larynx, both guttural pouches and the cervical trachea should be noted.

The next stage of dissection is to open the abdominal cavity, by a midline incision from paralumbar region down the ventral midline and along the rib margin. This exposes the right abdominal contents, and also then allows accurate visualisation of the diaphragm. The diaphragm should be domed cranially (Fig. 12), and should be inspected for any lesions such as fibrosis, adhesions to abdominal viscera, or hemorrhages. Herniation of abdominal contents into the thorax should be obvious, perforations or tears will be apparent on the left side of the diaphragm, but from this approach the right side of the diaphragm is unable to be assessed until the abdominal viscera are completely removed.



Figure 12. View of the diaphragm from the left side of the abdomen. The spleen and a lobe of the liver are evident in the foreground. The diaphragm is domed cranially. - To view this image in full size go to the IVIS website at www.ivis.org . -

The next phase of dissection is to perforate the diaphragm, making a keyhole incision at the diaphragmatic attachment to the ribs, using a sharp knife or scalpel. Normally, thoracic contents will be under negative pressure compared to atmospheric pressure, and air will be heard rushing into the thorax, accompanied by relaxation of the diaphragm back into the abdomen. In cases of pneumothorax, or severe pleuritis, where the thorax is not under negative pressure, the diaphragm may appear flaccid or domed into the abdomen. In order to review the lungs intact, it is important that the initial incision through the diaphragm is along the costal margin and not centrally. Perforation of the diaphragm centrally will almost invariably lead to laceration of the lungs. Once the diaphragm has been perforated, this costal incision should be extended from the level of the vertebra along the lateral attachments of the diaphragm to the sternum. At this point, the lungs can be visualised and an assessment for

pleural disease made (Fig 13).



Figure 13. Dissection of the costal muscular attachments of the diaphragm illustrating the left side of the thorax. Pleural surfaces, left lung, left side of the diaphragm and spleen are visible. - To view this image in full size go to the IVIS website at www.ivis.org . -

After dissection of the musculature over the left thoracic wall, ribs are sectioned using large bone cutters adjacent to the vertebral bodies dorsally and adjacent to the sternum ventrally. In doing so, the left thoracic wall is completely freed from the animal and can be removed. After assessment of the inner surfaces of the left thoracic wall for evidence of pleural disease, this can either be discarded or, in field postmortems, the inside aspect of the ribs can be used as a satisfactory sterile surface for temporary storage of specimens while the postmortem proceeds (Fig. 14, Fig. 15).



Figure 14. Normal left thoracic wall viewed from the pleural surface. - To view this image in full size go to the IVIS website at www.ivis.org . -



Figure 15. Typical in situ view of the left lung and the pericardium. Terminal hemorrhage is present in the cranial region of this lung. This is the "display stage" of dissection, for the respiratory tract. - To view this image in full size go to the IVIS website at www.ivis.org . -

The lungs are then visible for inspection and if occluding the trachea has been successful, there should be a uniform pale pink colour to the upper lung with only a few ml of clear yellow pleural fluid (Fig. 16, Fig. 17 and Fig. 18).



Figure 16. Typical appearance of normal lung prior to release of the tracheal clamps. - To view this image in full size go to the IVIS website at www.ivis.org . -



Figure 17. Typical appearance of normal lung following release of the tracheal clamps and collapse to minimal volume. - To view this image in full size go to the IVIS website at www.ivis.org . -



Figure 18. Closer view of normal lung while still inflated. The spleen lies to the right. - To view this image in full size go to the IVIS website at www.ivis.org . -

This concludes the "display stage of dissection", and at this point in the process, the tongue has been dissected from the mandible, enabling review of the oral and pharyngeal tissues. The esophagus along with trachea remain attached to the tongue and are available for review, and the right lung is visible in the thorax. At this stage, the objectives for postmortem evaluation for the respiratory tract should be reviewed, and if samples for microbiologic investigation have not already been taken, this is the most appropriate time to procure them, when there is minimal risk of contamination.

Removal of the Lower Respiratory Tract

Removal of the lower respiratory tract in large horses may require considerable strength, particularly if the lungs are filled

with exudate or infiltrates. By grasping the respiratory tract by the trachea at the level of the thoracic inlet, and applying tension to lift this out of the cadaver, anterior mediastinal tissues can be dissected free from the thoracic inlet, and the right pleural cavity also visualised. However, because the right pleural cavity lies ventral with this approach, fluids from the left pleural cavity empty into the right side and visualisation of the right pleural cavity is often impaired. Ventral mediastinal attachments are removed including those adjacent to the pericardium, a ligature is placed around the esophagus as it enters the diaphragm to prevent escape of ingesta from the stomach, and both the posterior vena cava and aorta are severed at the level of the diaphragm. The dorsal mediastinal attachments are separated so that the aorta is included. There are fibrous ligaments between the diaphragmatic lobes of the lung and the mediastinum caudal to the heart, and if these are not carefully sectioned, the lung parenchyma in this region will tear when tension is placed on the respiratory tract to lift it from the thorax. Once these ligaments are sectioned, the thoracic contents should be free within the thoracic cavity and can be lifted from the cadaver (Fig. 19, Fig. 20).



Figure 19. View of the entire respiratory tract removed from the cadaver. - To view this image in full size go to the IVIS website at www.ivis.org . -



Figure 20. Closer view of both lungs once removed from the thorax. In this case multiple sites of agonal hemorrhage are present and are common changes in the lungs of horses that are euthanised. - To view this image in full size go to the IVIS website at www.ivis.org . -

Because it is technically difficult to dissect the ventral mediastinal tissues away without rupturing the pericardial sac, it is best to open the pericardium while the thoracic contents are *in situ* in order to evaluate pericardial fluid.

Evaluation of the Tongue, Pharynx and Larynx

At this stage tongue, pharynx, larynx, and all structures distal to these in the respiratory tract have been removed and can be evaluated. For this part of the respiratory tract, the process of evaluation does not differ from the pathologic investigation of any other organ system. For solid structures, palpation and sectioning to allow visualisation of any lesions hidden beneath the surface are the usual approaches. For hollow structures, sectioning longitudinally to allow visualisation is the most useful approach. For the tongue and oropharynx, palpation and sectioning may rarely lead to identification of lesions, but commonly, inflammatory lesions are best identified by the accumulation of exudate adherent to mucosal surfaces. The volume of lymphoid tissue present in the pharyngeal region is variable, and lymphoid hyperplasia is a common disorder in young racehorses. For examples of oropharyngeal disease, see Fig. 21, Fig. 22 and Fig. 23.



Figure 21. Severe palatoschisis (cleft palate) in a foal. - To view this image in full size go to the IVIS website at www.ivis.org . -



Figure 22. Multifocal necroulcerative stomatitis in a horse. The condition is Noma, an uncommon condition in debilitated horses which develop rapidly expanding lesions associated with massive infection of necrotic tissue with opportunist anaerobes. - To view this image in full size go to the IVIS website at www.ivis.org . -



Figure 23. Multiple raised areas of pharyngeal nodular hyperplasia of tonsillar lymphoid tissues. - To view this image in full size go to the IVIS website at www.ivis.org . -

Although structural abnormalities may be detected in the oropharyngeal region in horses including abnormalities of soft palate, epiglottic size and shape, mucosal cysts in the region of epiglottis and pharynx, distorted and thickened cartilages with chondritis of the larynx, and cricoarytenoid muscle atrophy in cases of unilateral roarers, many disorders of the oropharynx in racehorses are functional and are not necessarily associated with obvious gross changes. A thorough postmortem evaluation of these tissues in cases where functional derangements are suspected should probably include an evaluation of glossopharyngeal and vagus nerves, but this is not routinely done in standard postmortem practice of horses. The problem is further compounded by postmortem collapse of the soft tissues around the pharynx after death, so that prolapse of soft tissues into the lumen of the oropharyngeal region is usual and cannot be interpreted accurately. For examples of guttural pouch and laryngeal disease, see Fig. 24, Fig.25, Fig. 26, Fig. 27, Fig. 28, Fig. 29, Fig. 30 and Fig. 31.



Figure 24. Acute pulmonary edema with blood tinged foam present at the level of the larynx. Such severe edema is associated with death, but may not be of pathologic significance in animals killed by barbiturate overdose. The distortion of the epiglottis is probably the consequence of chondritis, but is not significant when present only to this degree. - To view this image in full size go to the IVIS website at www.ivis.org . -



Figure 25. Supra-laryngeal streptococcal abscess causing dysphagia and respiratory noise. - To view this image in full size go to the IVIS website at www.ivis.org . -



Figure 26. Laryngeal amyloidosis illustrating swollen, inflamed and bleeding areas. The condition is relatively uncommon. - To view this image in full size go to the IVIS website at www.ivis.org . -

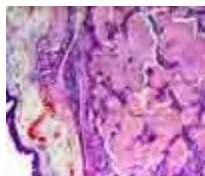


Figure 27. Histologic view of amyloidosis. In horses, intractable hemorrhage from the upper respiratory tract is usual. Generally, amyloid is of the inflammatory type, although the circumstances that lead to it developing only in particular animals remains unclear. - To view this image in full size go to the IVIS website at www.ivis.org . -



Figure 28. Laryngeal asymmetry associated with unilateral hemiplegia. - To view this image in full size go to the IVIS website at www.ivis.org . -



Figure 29. External laryngeal appearance illustrating severe unilateral (top) cricoarytenoid muscle atrophy. - To view this image in full size go to the IVIS website at www.ivis.org . -



Figure 30. Normal guttural pouch. A few tiny petechia are commonly present in the mucosa of the guttural pouch as an agonal change. - To view this image in full size go to the IVIS website at www.ivis.org . -



Figure 31. Guttural pouch empyema showing cores of caseous necrotic material. - To view this image in full size go to the IVIS website at www.ivis.org . -

Evaluation of the Tracheobronchial Tree

Prior to opening the trachea by the sectioning of the trachealis muscle dorsally, the external appearance of these large airways should be assessed. Normally the tracheal cartilage rings are a rounded C-shape, and are springy to palpation. Lesions external to the airway are easily noted on routine dissection, but it takes some experience to recognise changes in the springiness of the cartilage rings or alterations in shape. In animals with mural obstructive defects or degeneration of tracheal cartilages, generally there is a loss of tone of the cartilage rings, reflected as excessive flattening of the tracheal profile. Mural or extramural causes for respiratory disease in horses are unusual, and most abnormalities in the tracheobronchial tree reflect inflammatory processes. Typically in these cases, there is exudate in the airway, the character of which depends on the type of inflammatory process. Catarrhal to mucopurulent exudates are the most common, but flecks of blood or sanguineous edema fluid are common in horses that die during racing. A non-specific change common in the tracheobronchial tree is submucosal congestion, and may be so intense as to appear hemorrhagic. However, careful evaluation will allow discrimination, because with postmortem congestion (Fig. 32), digital pressure will cause blanching of the affected area, and the mucosa is intact.

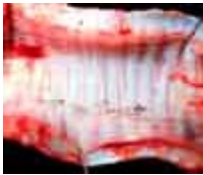


Figure 32. Normal appearance of the trachea showing postmortem congestion of submucosal vessels in between cartilage rings. - To view this image in full size go to the IVIS website at www.ivis.org . -

Ideally, a thorough investigation of the tracheobronchial tree should include dissection of all the major branches of the bronchial tree. In practice, this rarely done, and if 6 to 8 major bronchial airways are followed to their distal extremities, this is usually adequate to gain a reliable impression as to the health of the major airways, provided major bronchi from both cranial and caudal aspects of the lung are dissected. (Fig. 33, Fig. 34, Fig. 35, Fig. 36, Fig. 37 and Fig. 38).



Figure 33. Severe pulmonary edema with frothy fluid entirely filling the tracheal lumen. - To view this image in full size go to the IVIS website at www.ivis.org . -



Figure 34. Tracheobronchial disease is typically that involving the mucosa and lumen. This is an example of a rare mural disease. In this instance degeneration of tracheal and bronchial cartilages has led to tracheal distortion and narrowing. - To view this image in full size go to the IVIS website at www.ivis.org . -



Figure 35. Same condition as in Figure 34, illustrating occlusion and distortion of bronchi due to cartilaginous degeneration. - To view this image in full size go to the IVIS website at www.ivis.org . -



Figure 36. Same condition as in Figure 35, illustrating distorted abnormal bronchi and surrounding areas of lung collapse. - To view this image in full size go to the IVIS website at www.ivis.org . -



Figure 37. Bronchial rhabdomyoblastoma causing bronchial obstruction. Tumours of the respiratory tract are rare in horses. Original photograph by Dr Roger Breeze, during his appointment at Washington State University. - To view this image in full size go to the IVIS website at www.ivis.org . -



Figure 38. Bronchiectasis and obstruction with mucopurulent exudates in a chronically heavy horse. Bronchiectasis is less common in horses than cattle but does occur sporadically in cases of COPD. - To view this image in full size go to the IVIS website at www.ivis.org . -

Assessment of the Peripheral Lung

Once lungs are removed from the thorax, both lung fields are visualised, and ready for analysis. Removal of the clamps from the trachea should cause the lungs to collapse further, and a failure to do so generally indicates the presence of lung disease. However, in autolysed cadavers, lung collapse may not occur. The lung parenchyma represents one of the most difficult tissues in the body to examine grossly. Its appearance is greatly influenced by the state of inflation, the amount of blood, the degree of preservation, and by lung disease. It is one of the few tissues where pathologists must rely more on palpation than appearance for clues as to the presence of lung disease. Hyperinflated or emphysematous lungs appear pale, swollen, and are soft and easily distorted by palpation. (Fig. 39).



Figure 39. Appearance of normal lung, clamped at residual volume. - To view this image in full size go to the IVIS website at www.ivis.org . -

Conversely, atelectic lungs are rubbery to firm, and if completely airless, are red to plum coloured. (Fig. 40 and Fig. 41).



Figure 40. Severe diffuse atelectasis. The lung is reduced in size, airless, plum, coloured and rubbery rather than firm. - To view this image in full size go to the IVIS website at www.ivis.org . -

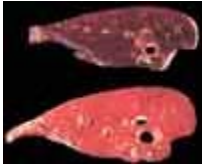


Figure 41. Comparison of atelectatic (upper) and normal (lower) sections of lung postmortem congestion of the lower lung may develop a similar colour to atelectatic lung but on transverse section, as shown here, will typically ooze blood and edema fluid. - To view this image in full size go to the IVIS website at www.ivis.org . -

Pulmonary edema is associated with pale, wet turgid lungs that fail to collapse, and generally frothy stable foam exudes from cut lung surfaces and is present within the airways. (Fig. 42 and Fig. 43).



Figure 42. Severe pulmonary edema with serous effusion. In this case, the edema is both evident interstitially and flooding alveoli, and was associated with bolus administration of barbiturate. - To view this image in full size go to the IVIS website at www.ivis.org . -



Figure 43. Cross section of edematous lung illustrating discharge of stable foam from larger airways. - To view this image in full size go to the IVIS website at www.ivis.org . -

Acute hemorrhage appears as red to black often confluent firm areas of lung (Fig. 44 and Fig. 45) and in general, airways leading to affected regions contain blood.



Figure 44. Scattered red to black foci in the anterior lung associated with acute hemorrhage. - To view this image in full size go to the IVIS website at www.ivis.org . -



Figure 45. Multiple foci of acute subpleural hemorrhage. - To view this image in full size go to the IVIS website at www.ivis.org . -

Areas of chronic hemorrhage generally are poorly circumscribed, firm to fibrous regions that are discoloured, red-rust coloured, brown or grey, depending on the amount of connective tissue deposition and whether or not mineralisation is present. (Fig. 46 and Fig. 47).



Figure 46. Typical features of chronic exercise-induced pulmonary hemorrhage (EIPH). There are bilateral, symmetrical fibrotic and siderotic areas along the dorsal aspects of both lungs. - To view this image in full size go to the IVIS website at www.ivis.org . -



Figure 47. Closer view of Figure 45. The brown discolouration is caused by accumulated iron pigments as a result of repetitive episodes of hemorrhage. - To view this image in full size go to the IVIS website at www.ivis.org . -

The distribution of lesions is important in discriminating between different forms of pneumonia. Most bronchopneumonias are cranioventral in distribution, contain areas of parenchymal collapse, and typically have mucopurulent to suppurative exudates within airways. Exogenous lipid pneumonias have a similar distribution, and if uncomplicated by secondary sepsis, appear as swollen, pale, yellow to grey, waxy areas of lung. Gangrenous pneumonias also have a cranioventral distribution commonly, but typically are associated with grey to black necrotising lung lesions, pronounced fetid smell and severe pleuritis. (Fig. 48, Fig. 49 and Fig. 50).



Figure 48. Gangrenous pneumonia. There is typically putrid odour, marked pleural effusion and toxemia. The distribution is often cranioventral lung fields. - To view this image in full size go to the IVIS website at www.ivis.org . -



Figure 49. Gangrenous pneumonia, cross section, illustrating cavitation of lung tissue due to necrosis, consolidation with exudate and lung collapse. - To view this image in full size go to the IVIS website at www.ivis.org . -



Figure 50. Severe fibrinosuppurative pleuritis with adhesions between thoracic wall and lung. A ruptured abscess is present near the centre of the field and in this case probably initiated the pleuritis. - To view this image in full size go to the IVIS website at www.ivis.org . -

Acute interstitial pneumonias, such as those associated with Gram negative septicemia's and acute viral infections in foals often produce blotchy, edematous, swollen lungs (Fig. 51) with scattered, variably sized hemorrhages.



Figure 51. Severe pulmonary edema and pleural effusion secondary to anaphylaxis. - To view this image in full size go to the IVIS website at www.ivis.org . -

Upon section, lungs often ooze blood-stained fluid, but major airways are generally clear. In cases of chronic interstitial and bronchointerstitial pneumonia, often caudal lung lobes are mostly affected. These have variable regions of either atelectasis or hyperinflation and affected lungs regions are often pale, firmer than normal, and may have pleural adhesions. (Fig. 52 and Fig. 53).



Figure 52. Chronic interstitial pneumonia associated with *Rhodococcus equi* infection. The affected areas of lung are firm, swollen and pale. - To view this image in full size go to the IVIS website at www.ivis.org . -



Figure 53. Cross section of lungs with irregular areas of interstitial pneumonia associated with *R. equi* infection. - To view this image in full size go to the IVIS website at www.ivis.org . -

When bronchiolar injury is significant, lesions may be seen radiating away from small airways, best identified with cross-sections of lung parenchyma. (Fig. 54 and Fig. 55).



Figure 54. Cross section of lung illustrating bronchiolar pneumonia. Larger airways remain unaffected but lesions can be seen radiating from bronchioles into adjacent lung parenchyma. Pale areas of necrosis and exudation alternate with adjacent areas of lung collapse and congestion. Most cases of bronchiolar pneumonia in horses are viral in origin. - To view this image in full size go to the IVIS website at www.ivis.org . -

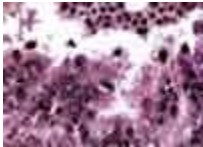


Figure 55. Histopathology of necrotising bronchiolitis associated with adenoviral infection in a foal. - To view this image in full size go to the IVIS website at www.ivis.org . -

Because of the large lung size, identifying small lung lesions deep to the pleura in horses may be difficult, and careful palpation of the entire lung is necessary. Irregular regions of discolouration occur commonly as a postmortem change in horses. Discoloured areas are not reliable indicators for good sampling sites for histopathology or microbiology. Therefore, if abnormalities can be detected by palpation, these are preferred to those where only visible changes are evident. For experimental studies, fixation of the entire lung in a state of inflation is desirable, but for routine diagnostic work this is impractical. Because of the existence of subsegmental collateral ventilatory channels in horse lungs, it is not possible to perfuse a sublobar bronchus and uniformly inflate an entire segment of lung. However, by injecting formalin into a distal airway, a partially expanded and well fixed sample for histopathology may be obtained. Due to the large size of the lungs, the effects of postmortem congestion and gravitational compression means there are distinct differences between dorsal and ventral and left and right lung fields in the typical postmortem specimens from the lung. Therefore, a comprehensive sampling technique must include both lung fields, samples derived from cranial, middle and caudal aspects of the lung, as well as samples derived from dorsal, middle and ventral aspects (Fig. 56).



Figure 56. Schematic of sampling sites for a survey of lung disease where no gross evidence of lesions is evident. From transverse sections through each lung, samples are taken in order that comparisons can be made:

- between dorsal, middle and ventral aspects (samples A1, B1, C1 with A2, B2, C2 and A3, B3, C3);
- between cranial, middle and caudal aspects (samples A1, A2, A3 with B1, B2, B3 and C1, C2, C3);
- between subpleural, midparenchymal and centrally (peribronchial) (samples A1, B2, C3 with A2, B3, C1 and A3, B1, C2).

- To view this image in full size go to the IVIS website at www.ivis.org . -

Pleural Disease

Pleural disease in horses is usually the consequence of sepsis, but is not always accompanied by obvious signs of lung disease. Pleuritis in horses is usually characterised by remarkable fluid accumulation, fibrin exudation and corresponding lung collapse (Fig. 57).



Figure 57. Acute fibrino purulent pleuritis. - To view this image in full size go to the IVIS website at www.ivis.org . -

Often multiple microbial pathogens can be recovered on culture, especially if pleuritis is associated with gangrene or lung abscessation (Fig. 58 and Fig. 59).



Figure 58. Subacute mixed bacterial septic pleuritis associated with pneumonia and lung abscessation. - To view this image in full size go to the IVIS website at www.ivis.org . -



Figure 59. Parietal pleura illustrating appositional lesions from the same case (Figure 56). In this case lung abscesses contained *Actinobacillus equuli*, micrococci and anaerobes. Necrosis of tissue had allowed the abscess contents into the pleural cavity. - To view this image in full size go to the IVIS website at www.ivis.org . -

Chronic fibrous scars are common on the pleural surfaces of the lungs of older horses and are sometimes associated with tough fibrous adhesions to the thoracic wall. (Fig. 60).

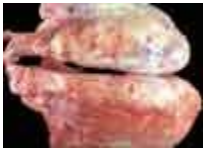


Figure 60. Chronic pleural scarring without adhesions to the thoracic wall. Scars in this case involve mainly the dorsal and lateral aspects of the lungs. The lungs are from an aged horse with a long history of severe chronic obstructive pulmonary disease (COPD). - To view this image in full size go to the IVIS website at www.ivis.org . -

This suggests that many horses recover from bouts of pleuritis and localized regions of pleural scarring do not seem to be clinically important. For examples of pleural disease, see Fig. 61, Fig. 62, Fig. 63, Fig. 64, Fig. 65, Fig. 66, Fig. 67, Fig. 68, Fig. 69, Fig. 70, Fig. 71, Fig. 72, Fig. 73 and Fig. 74.



Figure 61. Anomalous lung development. This condition, broncho-pulmonary dysplasia is rare in horses and when this is severe leads to death in the newborn. Alveolar development fails to take place and the lung tissue is comprised of solid, glandular or cystic parenchyma and poorly developed airways. - To view this image in full size go to the IVIS website at www.ivis.org . -



Figure 62. Neonatal pulmonary atelectasis and edema associated with a large interventricular septal defect of the heart. - To view this image in full size go to the IVIS website at www.ivis.org . -



Figure 63. Closer view of Figure 60 illustrating atelectasis, with marked subpleural and interstitial edema. - To view this image in full size go to the IVIS website at www.ivis.org . -



Figure 64. Chronic bronchopneumonia in a foal caused by *Rhodococcus equi* infection. There are abscesses and necrogranulomas present in the parenchyma. - To view this image in full size go to the IVIS website at www.ivis.org . -



Figure 65. Cross-section of the lungs in Figure 62. In younger animals *R. equi* often causes bronchopneumonia with development of residual abscesses and granulomas. - To view this image in full size go to the IVIS website at www.ivis.org . -



Figure 66. Histopathology of chronic granulomatous interstitial pneumonia caused by *R. equi*. In some animals areas of abscessation and interstitial pneumonia may co-exist within the same lung. - To view this image in full size go to the IVIS website at www.ivis.org . -

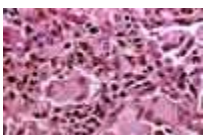


Figure 67. Detail from Figure 64, illustrating granulomatous pneumonia with prominent giant cells, macrophages lymphocytes and plasma cells. Generally large numbers of *R. equi* organisms are present and tissue Gram stains allow ready identification. - To view this image in full size go to the IVIS website at www.ivis.org . -



Figure 68. Not all granulomatous interstitial pneumonias of horses are caused by *R. equi* and this histopathology is from a case of avian tuberculosis. - To view this image in full size go to the IVIS website at www.ivis.org . -

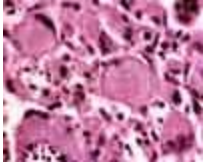


Figure 69. Detail of Figure 66, illustrating a similar tissue response as seen in Figure 65. However, Langhans giant cells in this case contained large numbers of acid-fast bacilli. Other causes for granulomatous pneumonias include foreign materials such as oil and silica dust, and mycotic or protozoal infections, particularly in foals. - To view this image in full size go to the IVIS website at www.ivis.org . -



Figure 70. Distinctive histopathology of *Pneumocystis carynni* infection. Generally affected animals are immuno-compromised. There is a mild lymphocyte-rich infiltrate around vessels and interstitially, but alveolar lumens are flooded with cell poor proteinaceous edema fluid in which ghost outlines of pneumocystis can generally be seen on routine staining. Silver stains are helpful in confirming the diagnosis. - To view this image in full size go to the IVIS website at www.ivis.org . -

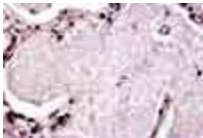


Figure 71. Detail of Figure 68 (*Pneumocystis* infection). - To view this image in full size go to the IVIS website at www.ivis.org . -

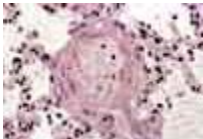


Figure 72. Lysis of cells, edema and hemorrhage of a pulmonary blood vessel. The change is a common artefact caused by the caustic effects of concentrated barbiturate injection used to euthanase horses. - To view this image in full size go to the IVIS website at www.ivis.org . -



Figure 73. Chronic peribronchiolitis with minimal parenchymal changes. The lesion is commonly associated with chronic obstructive pulmonary disease (COPD) but is not diagnostic and many older horses without COPD may have similar peribronchiolar lesions. - To view this image in full size go to the IVIS website at www.ivis.org . -



Figure 74. Chronic peribronchiolitis with mucopurulent exudates in airways extending into adjacent alveoli. Chronic obstructive pulmonary disease (COPD) case. In acute exacerbations, neutrophilic rather than eosinophilic infiltrates are common in the exudates that accumulate. In more chronic cases, a variety of tissue changes may be present, including many of the stigmata of asthma in humans; peribronchiolar fibrosis, smooth muscle hyperplasia, chronic inflammation, mucosal hyperplasia and epithelial metaplasia, mucus obstruction, alveolar scarring and emphysema. - To view this image in full size go to the IVIS website at www.ivis.org . -

Evaluation of the Nasal Cavity

After removal of the head from the cadaver, the top of the calvarium is sawn free, and the brain removed. In the laboratory, bisection of the skull along the midline to expose the nasal cavity is a simple matter, but in field postmortems this requires a stout saw and a strong arm. Once the skull has been bisected, (Fig. 75), the cartilaginous portion of the nasal septum is easily removed, allowing visualisation of the nasal turbinates (Fig. 76).



Figure 75. Bisection of the skull, nasal septum still intact. - To view this image in full size go to the IVIS website at www.ivis.org . -



Figure 76. Normal appearance of nasal turbinates after removal of the septum. - To view this image in full size go to the IVIS website at www.ivis.org . -

Tissues may require further dissection to evaluate the sinuses, except for the frontal sinus which is easily visualised after bisection of the skull (Fig. 77).



Figure 77. Inspection of the sinuses. - To view this image in full size go to the IVIS website at www.ivis.org . -

In postmortem specimens, typically the nasal mucosa is intensely congested, appearing dark-red to almost black. This is generally of no significance, unless there are mucosal lesions accompanying this change. Exudates within the nasal cavity, or focal lesions leading to destruction of turbinates, are the usual indicators of nasal disease. The most common disorders include acute infectious disease, although these are generally not sufficiently severe to cause the animal's death. Chronic diseases such as glanders leave distinctive stellate scars in the nasal mucosa, but many acute bacterial and viral infections are not grossly distinctive and require additional microbiologic methods for confirmation of diagnosis. Other pathologic changes common to the nasal cavity include bone cysts, ethmoid hematomas, abscesses extending from the sinuses, traumatic lesions resulting from the passage of stomach tubes and instruments, and developmental anomalies. Neoplastic diseases of the respiratory tract in horses are extremely rare. Histologic evaluation of the structures of the nasal cavity and sinuses also needs to account for significant regional variations in normal tissue structure. In areas of high airflow, the epithelium varies from transitional to stratified squamous, the ethmoid mucosa is specialised, and the respiratory epithelium over the remainder of the nasal cavity is a typical ciliated pseudostratified epithelium. As with the lower respiratory tract, provided a routine sampling procedure is used, then histopathology is little different to that for the respiratory tract of any other species. For examples of nasal disease, see Fig. 78, Fig. 79, Fig. 80, Fig. 81, Fig. 82, Fig. 83 and Fig. 84.



Figure 78. Chronic granulation tissue obstructing the nasal cavity and causing turbinate atrophy. - To view this image in full size go to the IVIS website at www.ivis.org . -



Figure 79. Mass of granulation tissue reflected from the nasal cavity. - To view this image in full size go to the IVIS website at www.ivis.org . -



Figure 80. Maxillary turbinate bone cyst. The bone cyst displaces surrounding turbinates and is filled with degenerate blood. - To view this image in full size go to the IVIS website at www.ivis.org . -



Figure 81. Nasal granulomata associated with conidiobolus infection. Illustration taken from Miller RI [2]. - To view this image in full size go to the IVIS website at www.ivis.org . -



Figure 82. Nasal hematoma secondary to trauma. - To view this image in full size go to the IVIS website at www.ivis.org . -



Figure 83. Ethmoid hematoma. The lesion is associated with multifocal areas of granulation tissue, hemosiderosis and fibrosis, and repeated episodes of hemorrhage. The lesion often expands leading to progressive turbinate destruction. The brown area is comprised of granulation tissue rich in degraded iron pigments. - To view this image in full size go to the IVIS website at www.ivis.org . -



Figure 84. Hemorrhagic cystic cavity lined by granulation tissue that replaces normal turbinate tissue; ethmoid hematoma. - To view this image in full size go to the IVIS website at www.ivis.org . -

For further reading, see references [3] and [4]

References

1. Sack WO, Habel RE. Rooney's Guide to Dissection of the Horse. New York: Veterinary Textbooks, 1967.
2. Miller RI. Equine phycomycosis. *Compend Cont Edu*, 1983; 5(9):S472-S478.
3. Dungworth D. The respiratory system. In: Kennedy PC, Jubb KV and Palmer NC, eds. *Pathology of Domestic Animals*, Volume 2, 4th edition. San Diego: Academic Press, 1993; 539-698.
4. Lopez A. Respiratory system. In: Thomson RG, Carlton WW, McGavin D et al., eds. *Thomson's Special Veterinary Pathology*, 3rd edition. St. Louis: Mosby, Inc., 2000; 25-195.

All rights reserved. This document is available on-line at www.ivis.org. Document No. B0310.0403.

